Quantum Electronics **49** (6) 559–562 (2019)

https://doi.org/10.1070/QEL17033

Difference-frequency generation in a dual-wavelength semiconductor disk laser: Model with delayed feedback

Yu.A. Morozov, M.I. Balakin, L.A. Kochkurov, A.I. Konyukhov, M.Yu. Morozov

Abstract. **We have constructed a mathematical model of an intracavity difference-frequency generator based on a dual-wavelength semiconductor disk laser in the form of a time-delay dynamic system. Steady-state lasing (the equilibrium state of the dynamic system), its stability, and also transient dynamics after switching on the primary optical pump source are investigated. It is shown that the equilibrium state is stable in a wide range of parameters, which is of interest for possible applications of such a generator.**

Keywords: *nonlinear-optical interaction, difference-frequency generation, mid-IR range, semiconductor disk laser.*

1. Introduction

Continuous-wave difference-frequency generators and optical parametric oscillators can be successfully used in high-resolution spectroscopy [1]. Particularly promising are intracavity versions of these devices. After the development of a dual-wavelength vertical-external-cavity surface-emitting laser, or, as it is also called, a semiconductor disk laser [2], it became possible to design a compact mid-IR intracavity difference-frequency generator (ICDFG) on its basis (with an emission wavelength of about 16.5 μm) [3].

Previously, the prospects of an intracavity optical parametric oscillator (OPO) pumped by a semiconductor disk laser has been demonstrated in [4], where in a singly resonant OPO, pump, signal and idler had wavelengths of 1.05, 1.6 and 3.05 μm, respectively (the primary pump source was a 808 nm diode laser). One of the drawbacks of such a device is, in our opinion, the impossibility of significant convergence of the pump and signal wavelengths, since the cavities of these optical fields are separated using a dichroic beam splitter. In this case, a substantial increase in the idler wavelength is impossible.

The use of a common cavity for the pump and signal fields [3] eliminates this disadvantage. In addition, the approach formulated in [3] can be applied to produce both an OPO and an ICDFG. In this case, only the design of the gain mirror is changed, and the general scheme remains the same.

One of the factors that determine the suitability of the ICDFG for use in spectroscopy is the stability of steady-state lasing with regard to relatively small perturbations of this state. For a theoretical analysis of linear stability, a mathematical model is used that formalises the dynamic behaviour of the generator. Often, such a model involves the expansion of optical fields in cavity modes, so-called Slater normal mode expansion [5–9]. For out-of-phase modes (or if only one longitudinal mode is taken into account), this approach leads to a small change in the amplitudes of the fields on the time scale of a round-trip for the light in the cavity. At the same time, it should be noted that more rapid changes in the amplitude of the fields are not prohibited under strict electrodynamic consideration; these values should change little in the transient mode (or remain constant in the stationary oscillation mode in a high-Q cavity) only at neighbouring times separated by a time interval that is a multiple of the round-trip transit time for the light in the cavity.

To analyse faster oscillations of the field intensity and to study the effect of these oscillations on the stability of the steady state, we use the model of a time-delay dynamic system [10–13]. This model considers a laser in the form of coupled cavities, the optical fields are considered within a subcavity, and the influence of the external (main) cavity is taken into account in the form of multiple delayed reflections. In this paper, this model has been upgraded to take into account the effect of nonlinear-optical interaction on steady-state characteristics and system dynamics. Note that our model assumes that the amplitude of the light reflected from the external cavity is large compared to that in the subcavity. This fundamentally distinguishes our model from the well-known Lang–Kobayashi model [14], which, as is well known, takes into account small-level external reflections.

2. Derivation of a mathematical model

The schematic of the ICDFG in question is shown in Fig. 1. The basis of the device is a dual-wavelength semiconductor disk laser (SDL), which is also called a dual-wavelength vertical-external cavity surface–emitting laser [2]. The generator consists of a subcavity formed by a Bragg mirror and a reflecting face of the structure facing the external cavity. To provide the necessary reflection bandwidth, the Bragg mirror is made in the form of a double-band mirror (DBM). The volume of the subcavity is filled with a gain medium consisting of quantum wells (QWs) separated by barriers. Therefore, the subcavity is also called the gain mirror. The external (main) cavity is formed by the DBM on the one side and by an output

Yu.A. Morozov, M.Yu. Morozov Kotel'nikov Institute of Radio Engineering and Electronics (Saratov Branch), Russian Academy of Sciences, ul. Zelenaya 38, 410019 Saratov, Russia;
e-mail: yuri.mor@rambler.ru;
M.I. Balakin, L.A. Kochkurov Yuri Gagarin State Technical University of Saratov, ul. Politekhnicheskaya 77, 410054 Saratov, Russia;
A.I. Konyukhov N.G. Chernyshevsky Saratov State University, ul. Astrakhanskaya 83, 410012 Saratov, Russia

Received 4 April 2019
Kvantovaya Elektronika **49** (6) 559–562 (2019)
Translated by I.A. Ulitkin

spherical mirror on the other. This generator provides the simultaneous generation of short-wavelength (with a wavelength of 1.98 μm) and long-wavelength (2.25 μm) fields (in the terminology of parametric interaction, these fields are called pump and signal). As was already noted, the external cavity is common for the pump and signal fields. To ensure nonlinear optical interaction, accompanied by the difference-frequency generation (idler), a nonlinear quasi-phase-matched GaAs crystal is placed near the gain mirror (i.e., in the region where the power density of the pump and signal optical fields is the highest). Ider radiation with a wavelength of 16.5 μm is not resonant, i.e. it can freely exit through an external mirror.

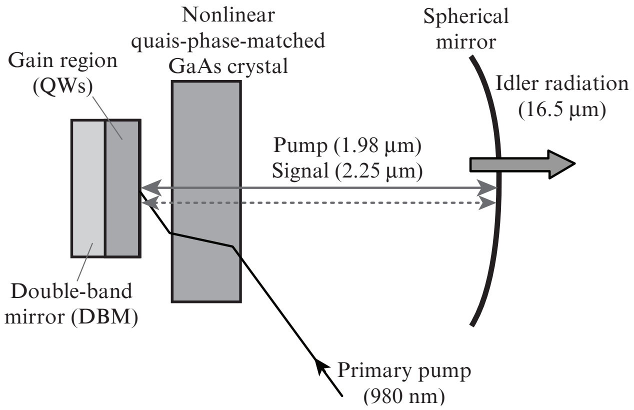

Figure 1. Schematic of the intracavity difference-frequency generator.

The gain mirrors of the ICDFG and a conventional SDL are significantly different. First, in the ICDFG gain medium, there are at least two clusters (sets) of QWs of different molar composition (shallow $Ga_{0.74}In_{0.26}Sb$ and deep $Ga_{0.7}In_{0.3}As_{0.06}Sb_{0.94}$) designed to generate the pump and the signal (Fig. 2). The carrier inversion in the QW is produced due to the absorption of the optical pump (primary pumping) in the barrier layers separating the QWs. In order to avoid competition for QW carriers belonging to different gain regions, these regions are separated from each other by a wide-gap blocking layer ($Al_{0.85}Ga_{0.15}As_{0.068}Sb_{0.932}$), which prevents the transport of carriers between them. Another distinctive feature, compared with the device of the gain region of a conventional (single-wavelength) semiconductor disk laser, is the arrangement of the QWs with respect to the spatial structure of the optical fields: the 'long-wavelength' QWs are located at the nodes of the short-wavelength field. At the same time, the coupling of optical fields due to the possible absorption of this radiation is minimal, but each of the sets of QWs is located in the antinodes of its own field to ensure the highest possible gain.

The key to constructing a mathematical model is the consideration of reflections in the structure of the laser (Fig. 3). Here r and R are the moduli of the reflection coefficients of the gain and output mirrors, respectively; and $r_{\rm DBM}$ is the reflection coefficient of the DBM. A nonlinear crystal with a length L_c located near the gain mirror is shown in the scheme as a darkened area. As mentioned in the formulation of the problem, we consider the fields inside the gain mirror, and the influence of the external cavity is taken into account with the help of multiple reflections of the field. Then the effective reflection coefficient of the outer surface of the gain mirror can be written as

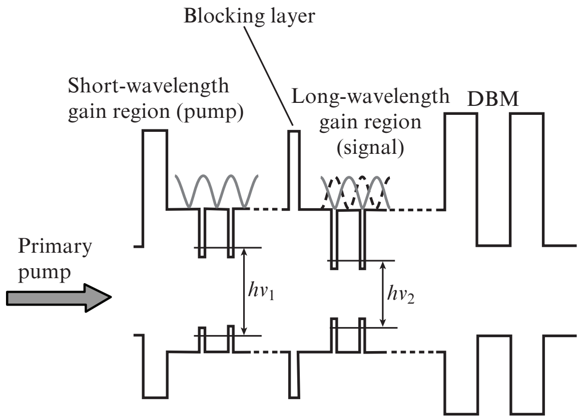

Figure 2. Energy diagram of the gain mirror for the ICDFG.

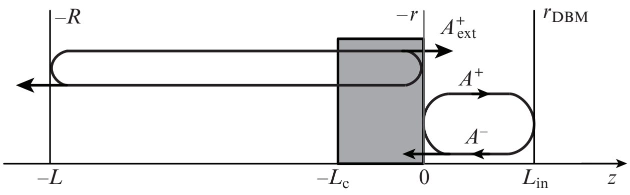

Figure 3. Reflections in the ICDFG structure.

$$r_{\rm eff} = \frac{A^+ + A^+_{\rm ext}}{A^-}, \tag{1}$$

where A^+ and A^- – are the amplitudes of waves propagating, respectively, in the positive and negative directions of the z axis (these quantities represent the optical fields in the subcavity without contribution of reflection from the external cavity); and $A^+_{\rm ext}$ is the complex amplitude of the reflections from the external cavity. When performing the summation of reflections in the external cavity, we obtain

$$r_{\rm eff} = r\left[1 - \chi\sum_{m=1}^{\infty}(R_{\rm eff}r)^{m-1}\frac{A^+(t-m\tau)}{A^+(t)}\exp(-{\rm j}\omega m\tau)\right]. \tag{2}$$

Here, $\chi = R_{\rm eff}(1 - r^2)/r$; ω is the angular frequency of the corresponding field; τ is the round-trip transit time for the light in the external cavity; and $A^+(t - m\tau)$ is a replica of the complex amplitude of the field $A^+(t)$, delayed by the time equal to m round trips of the light in the cavity. In two limiting cases: with $\chi \ll 1$ ($R_{\rm eff} \ll 1$) and $\chi \gg 1$ (due to $r \ll 1$, antireflection coating on the gain mirror), we can limit ourselves to considering only a single round-trip of the light in the external cavity. In the first case, the Lang–Kobayashi model [14] of weak coupling with external space is realised, and in the second, our model is used when the coupling with the external cavity is strong.

In formula (2), the $R_{\rm eff}$ value takes into account the contribution of both reflections from the external mirror and the effect of nonlinear-optical interaction in a nonlinear crystal:

$$R_{\rm eff1} = R[1 - \mu(f_2 + f_{2\tau})]^{1/2} \tag{3}$$

for the pump and

$$R_{\rm eff2} = R[1 + \mu(f_1 + f_{1\tau})]^{1/2} \tag{4}$$

for the signal radiation. Here, f_i corresponds to a one-sided photon flux of the pump ($i = 1$) and signal ($i = 2$) fields; hereafter, the value with the subscript τ refers to the moment of time delayed by the value of τ, that is, $f_{i\tau} = f_i(t - \tau)$. We assume that the pump and signal fields are represented by Gaussian beams with radii w_1 and w_2; it turns out that $\mu = 2\gamma/[\pi(w_1^2 + w_2^2)]$, where

$$\gamma = \frac{32Z_0}{n_1 n_2 n_3} d_{14}^2 \left(\frac{L_c^2}{\lambda_1 \lambda_2}\right) \hbar\omega_3. \qquad (5)$$

In (5), $Z_0 = 120\pi$ is the impedance of free space; $n_{1,2,3}$ are the refractive indices of the nonlinear GaAs crystal for the corresponding wavelengths; d_{14} is the element of the nonlinear susceptibility tensor; $\lambda_{1,2}$ are the wavelengths of the pump and the signal; and $\hbar\omega_3$ is the idler photon energy.

Using the approach formulated in [13], taking into account the above equations, we obtain the system of time-delay dynamic equations for the ICDFG in question:

$$\dot{s}_1 = \eta\left[(G_1 - 1) + \frac{1}{T}\left(\frac{s_{1\tau}}{s_1} - 1\right) - \frac{\delta}{T}(s_2 + s_{2\tau})\right]s_1,$$

$$\dot{s}_2 = \eta\left[(G_2 - 1) + \frac{1}{T}\left(\frac{s_{2\tau}}{s_2} - 1\right) + \frac{\delta}{T}(s_1 + s_{1\tau})\right]s_2, \qquad (6)$$

$$\dot{\nu}_1 = \sigma_1 - \nu_1 - G_1 S_1,$$

$$\dot{\nu}_2 = \sigma_2 - \nu_2 - G_2 S_2.$$

Here, the numbers of photons s_i and carriers ν_i are normalised to s_{i0} and $\nu_{i\text{th}}$, respectively, with $s_{i0} = \nu_{i\text{th}}/\eta$, where $\nu_{i\text{th}}$ is the threshold number of carriers in the ith gain region; $\eta = \tau_r/\tau_{ph}$ [τ_r and $\tau_{ph} = (\upsilon_g \alpha_s)^{-1}$ are the lifetimes of carriers and photons in the subcavity]; $T = 2\alpha_s L_{in}$ is the loss due to the round trip of the light of the cavity; and $\alpha_s = \alpha_{in} - (L_{in})^{-1}\ln[r_{DBM}(1 - r^2)R]$ is the loss coefficient in the subcavity. The gain G_i according to [15, 16] takes the form $G_i = 1 + G_{i0}\ln\nu$, where $G_{i0} = 4m_i G_{QW}/T$, m_i is the number of QWs in the ith gain region, and G_{QW} is the gain per one QW (we assume it to be the same for QWs of different molar compositions). The threshold number of carriers can be defined as $\nu_{i\text{th}} = m_i \pi w_{pp}^2 N_t \exp(1/G_{i0})$, where w_{pp} is the radius of the primary pump beam, and N_t is the surface density of carriers at transparency. The nonlinear interaction factor has the form $\delta_i = \mu a_{i0}/\tau_{in}$, where $\tau_{in} = 2L_{in}/\upsilon_g$ is the round-trip transit time of the light in the subcavity. The primary pump power, normalised to the threshold value, is denoted as $\sigma_i = P/P_{i\text{th}}$. The points above the variables in the left-hand sides of equations (6) mean differentiation by the normalised time t/τ_r.

3. Results of numerical simulation

Most calculations were performed with the following parameters of the device: $L = 30$ mm, $L_c = 5$ mm, $L_{in} = 5$ μm, $\lambda_1 = 1.98$ μm, $\lambda_2 = 2.25$ μm, $w_1 = w_2 = 80$ μm, $w_{pp} = 90$ μm, $d_{14} = 1.0\times10^{-4}$ μm V^{-1}, $n_1 \approx n_2 = 3.335$, $n_3 = 3.22$, $T = 0.025$, $\tau_r = 2\times10^{-9}$ s, $N_t = 1.45\times10^{12}$ cm^{-2}, and $G_{QW} = 2.0\times10^{-3}$ [16]. Each of the gain regions of the ICDFG contained five QWs. During the calculations, we assumed that the primary pump power is absorbed in equal parts in the gain regions.

Linear stability (i.e., stability with respect to small perturbations) of the steady state (otherwise, the equilibrium state of the dynamical system) was studied using the DDEBIFTOOL software package [17]. The characteristic equation of the system has an infinite number of roots, most of which can be grouped into two sets consisting of complex conjugate pairs:

$$\lambda_n^{(1,3)} = \text{Re}(\lambda_n^{(1)}) \pm \text{j}\,\text{Im}(\lambda_n^{(1)}),$$
$$\lambda_n^{(2,4)} = \text{Re}(\lambda_n^{(2)}) \pm \text{j}\,\text{Im}(\lambda_n^{(2)}). \qquad (7)$$

In addition, there is a countable number of pure real roots, but their values are much smaller in magnitude than the real parts of the roots of sets (7). Therefore, these real roots are not significant in determining the stability. The imaginary parts of roots (7), which, as is known, determine the frequency of oscillations of small deviations from the equilibrium state, are approximately in a multiple ratio with the intermode beat frequency, i.e. $\text{Im}(\lambda_n^{(1,2)}) \approx 2\pi n/\tau$. This relation fully agrees with the conclusions of the general theory regarding the structure of the roots of the characteristic equation for a time-delay dynamic system [18].

The calculations showed that in a wide range of practically interesting values of the ICDFG parameters and the pump, the real parts of roots (7) remain negative. In other words, the steady-state position of the dynamic system (6) is stable. This position is important for possible ICDFG applications in high-resolution spectroscopy systems.

To confirm the conclusion about the stability of the equilibrium state, we performed calculations of the establishment of a steady state with the values of the parameters given above and the primary pump parameter $\sigma_1 = \sigma_2 = 10$. Figure 4 shows the transient dynamics for the pump and the signal. In the calculations, we assumed that the primary pump power is switched on abruptly at time $t = 0$. It can be seen that to increase the radiation intensity to noticeable values, a time of several dozen carrier lifetimes τ_r or phonon lifetimes in the external cavity is needed (for the ICDFG with these parameters the lifetime is $\tau_{PH} \approx 2L/(cT) = 4\tau_r$). It also follows from Fig. 4 that the establishment of oscillations occurs through weakly decaying relaxation oscillations (the characteristic decay time is $\sim 1000\tau_r$). The form of these oscillations is complex: The inset shows a selected section of dynamic behaviour, with a period of oscillations approximately equal to the round-trip transit time $\tau = 0.1\tau_r$. In general, the establishment

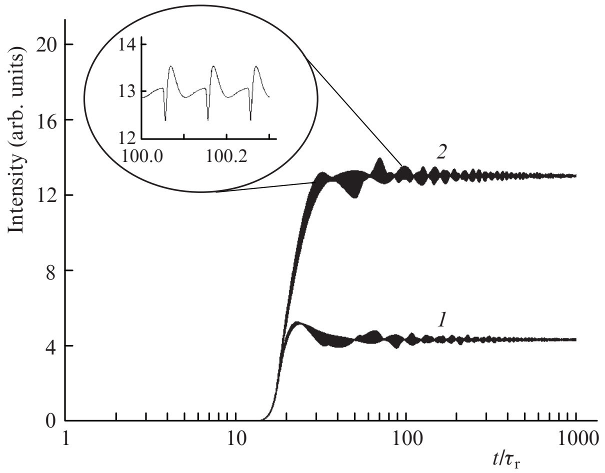

Figure 4. Dynamics of (*1*) the pump and (*2*) the signal in the transient mode of the ICDFG.

of an equilibrium state occurs as a result of a decaying process, which is characterised by the multi-scale characteristic times (there are fast oscillations with a characteristic time of the order of the round-trip transit time in the cavity with a slow change in the amplitude of these oscillations).

4. Conclusions

A system of rate time-delay differential equations for a difference-frequency generator based on a dual-wavelength semiconductor disk laser is formulated. The steady state (the equilibrium state of the dynamic system), its stability with respect to small perturbations, and the transient dynamics after the primary pump is turned on are calculated.

It is shown that the characteristic equation has an infinite set of roots, most of which can be grouped into complex conjugate pairs. The imaginary parts of the roots, which are the oscillation frequencies of small deviations from the equilibrium state, are separated from each other by the frequency of intermode beats in the cavity of the device. The real parts of the roots, the maximum of which determines the time needed to establish an equilibrium, are negative, i.e., the equilibrium state is stable (at least at the studied values of the parameters). This is an important finding for the intended use of the ICDFG in spectroscopy devices.

The transient dynamics of the ICDFG radiation confirms conclusions about the stability of the steady state. It is shown that the establishment of oscillations to a stationary value occurs slowly (on a scale of $1000\tau_r$), and the characteristic time of a change in the amplitude of oscillations in any selected short time interval is approximately equal to the round-trip transit time for the light in the cavity.

Acknowledgements. The work was performed at IREE RAS within the framework of the state task and was partially supported by the Russian Foundation for Basic Research (Project No. 18-08-00599-a).

References

1. Sorokina I., Vodopyanov K. (Eds.) *Solid-State Mid-Infrared Laser Sources* (Berlin, Heidelberg: Springer-Verlag, 2003).
2. Leinonen T., Morozov Y.A., Härkönen A., Pessa M. *IEEE Photon. Techn. Lett*., **17**, 2508 (2005).
3. Morozov Y.A. *Appl. Phys B*, **124**, 12 (2018).
4. Stothard D.J.M., Hopkins J.M., Burns D., Dunn M.H. *Opt. Express*, **17**, 10648 (2009).
5. Hodges S.E., Munroe M., Cooper J., Raymer M.G. *J. Opt. Soc. Am. B*, **14**, 191 (1997).
6. Debuisschert T., Raffy J., Pocholle J.P., Papuchon M. *J. Opt. Soc. Am. B*, **13**, 1569 (1996).
7. Turnbull G.A., Dunn M.H., Ebrahimzadeh M. *Appl. Phys. B*, **66**, 701 (1998).
8. Morozov Y.A. *J. Opt. Soc. Am. B*, **33**, 1470 (2016).
9. Siegman A.E. *Lasers* (California: University Science Book, 1986).
10. Park J.D., Seo D.S., McInerney J. *IEEE J. Quantum Electron.*, **26**, 1353 (1990).
11. Hui R.Q., Tao S.P. *IEEE J. Quantum Electron*., **25**, 1580 (1989).
12. van Tartwijk G.H.M., Lenstra D. *Quantum Semiclass. Opt*., **7**, 87 (1995).
13. Morozov Y.A., Leinonen T., Härkönen A., Pessa M. *IEEE J. Quantum Electron*., **42**, 1055 (2006).
14. Lang R., Kobayashi K. *IEEE J. Quantum Electron.*, **16**, 347 (1980).
15. Zory P.S. (Ed.) *Quantum-Well Lasers* (San Diego: Acad. Press, 1993).
16. Rattunde M., Schmitz J., Mermelstein C., Kiefer R., Wagner J., in *Mid-Infrared Semiconductor Optoelectronics. Springer Series in Optical Sciences* (London: Springer-Verlag, 2006) p. 131.
17. Engelborghs K., Luzyanina T., Roose D. *ACM Transactions on Mathematical Software*, **28**, 1 (2002).
18. Yanchuk S., Giacomelli G. *J. Phys. A: Math. Theor.*, **50**, 103001 (2017).